Supporting information

Partially Sulfurized Nickel-Cobalt LDH on CNT-coated Aramid Fiber for High-performance Yarn-shaped Supercapacitors

Yanzhi Fan [a], Zhen Yang [b], Xiao Han [b], Donyan Li [a], Minghui Yuan [a], Chen Liu [a], Junhao Jia [a], Xin Zhang [a], Huimin Zhang [a], Jun Yan [a], Ying Wang [a], Hong Li [a], Yongping Liao [a, *]

[a] School of Textile and Material Engineering, Dalian Polytechnic University, Dalian 116034, China
[b] Luthai Textile Co., Ltd., Zibo 255100, China
[*] Corresponding author, E-mail address: liaoyp@dlpu.edu.cn

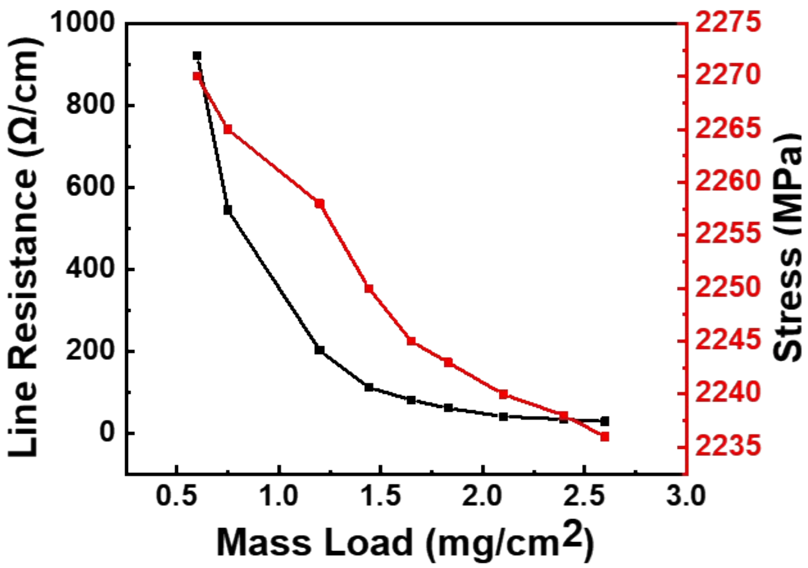

Fig. S1. Relationships between line resistance and strength and mass load of CNTs.

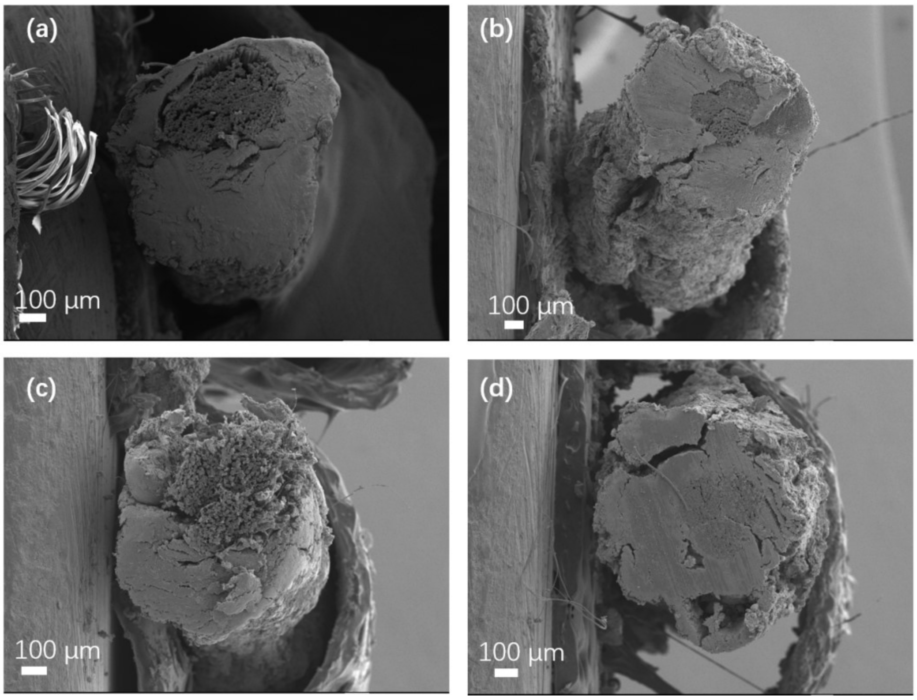

Fig. S2. The cross-sectional SEM images of (a) NiCo-LDH@CAY, (b) NiCo-LDH-S_1@CAY, (c) NiCo-LDH-$S_{1.5}$@CAY, (d) NiCo-LDH-S_2@CAY.

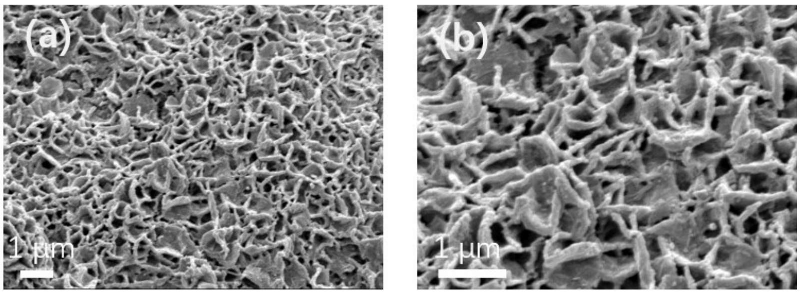

Fig. S3. Scanning electron microscope image of nickel-cobalt hydrotalcite after 5h of sulfurization

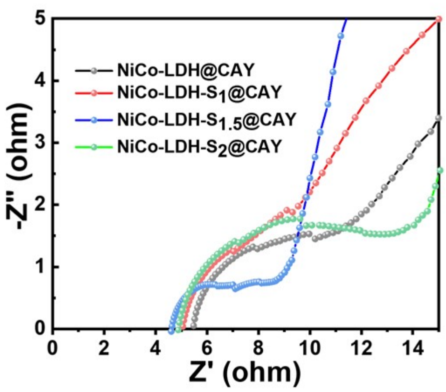

Fig. S4. The Nyquist plots of the four types in the high-frequency region (the magnified zone of Figure 4e).

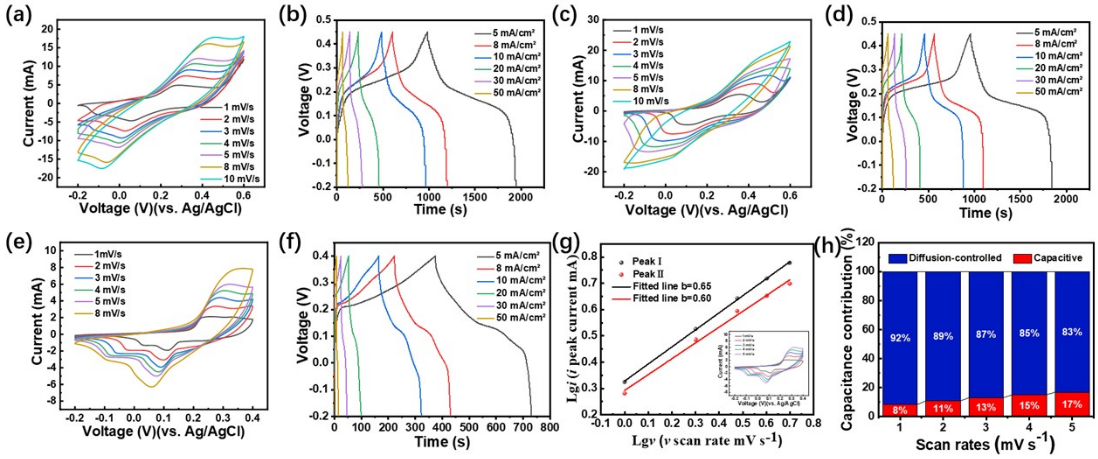

Fig. S5. (a) CV and (b) GCD curves of the NiCo-LDH-S_1@CAY composite electrode material at various scan rates and current densities, respectively. (c) CV and (d) GCD curves of the NiCo-LDH-S_2@CAY composite electrode material at various scan rates and current densities, respectively. (e) CV and (f) GCD curves of the NiCo-LDH@CAY composite electrode material at various scan rates and current densities, respectively. (g) The relationship between the peak current and the scanning rate of NiCo-LDH@CAY. (h) The detailed contributions of diffusion-controlled processes and surface capacity effect in NiCo-LDH@CAY.

Table S1. Equivalent circuit simulation values of the EIS results.

Electrode	Impedance values (Ω)		
	R_s	R_1	R_2
NiCo-LDH@CAY	5.32	4.42	20.19
NiCo-LDH-S_1@CAY	5.01	4.24	18.29
NiCo-LDH-$S_{1.5}$@CAY	4.27	1.12	2.19
NiCo-LDH-S_2@CAY	4.86	2.55	2.89

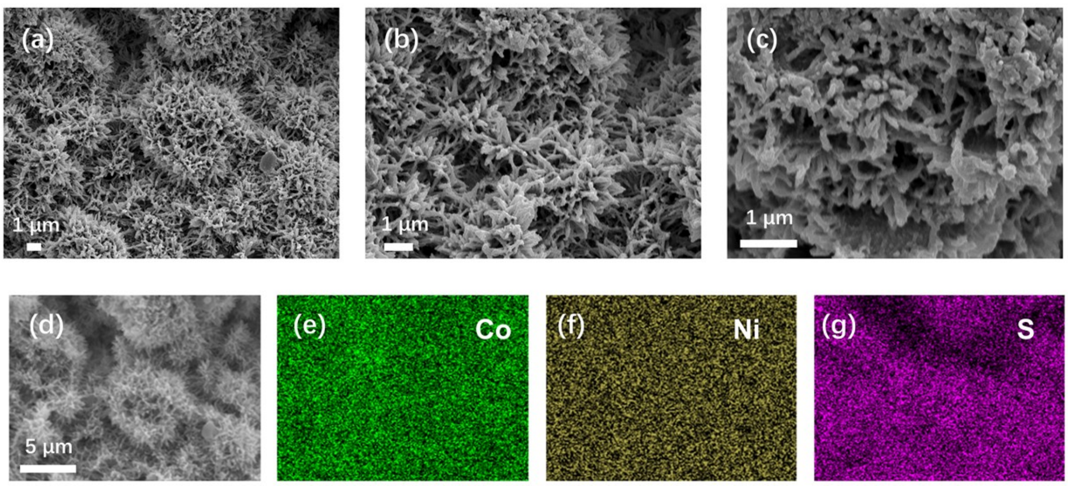

Fig. S6. (a-c) SEM images of post-cycling NiCo-LDH-$S_{1.5}$@CAY, (d) SEM image for (e-g) EDS mappings of the post-cycling sample.

Table S2. Comparison of the capacitance, energy density, and power density of the device with those in the literature.

Electrode materials	Current collector	Electrolyte	V	*i*	C_A	P_A	E_A
PPy nanotubes[1]	cotton yarn	PVA/H_2SO_4	1.8V	0.42 mA cm^{-2}	74.0 mF cm^{-2}	22.40 μW cm^{-2}	7.5 μWh cm^{-2}
Ni-Co LDH[2]	Ni/cotton yarn	PVA/KOH	0.75V	0.04 mA cm^{-2}	221 mF cm^{-2}	43.99 μW cm^{-2}	9.3 μWh cm^{-2}
Co_3O_4[3]	CNT yarn	PVA/H_2SO_4	0.8V	0.053 mA cm^{-2}	52.6 mF cm^{-2}	10 μW cm^{-2}	1.10 μWh cm^{-2}
NiO[3]	CNT yarn	PVA/H_2SO_4	0.8V	0.053 mA cm^{-2}	15.2 mF cm^{-2}	5 μW cm^{-2}	0.2 μWh cm^{-2}
NiCo-OH/ZnO-NR[4]	CNT-yarn	PVA/LiOH	/	/	/	117 μW cm^{-2}	1.38 μWh cm^{-2}
MoS_2/MnS/GR[5]	PI fibers	PVA/Na_2SO_4	1.0V	0.05 mA cm^{-2}	50.2 mF cm^{-2}	49.9 μW cm^{-2}	7.0 μWh cm^{-2}
NiCo2S4@Ni-Co LDH[6]	Au/cotton yarn	PVA/KOH	0.8V	0.4 mA cm^{-2}	37.2 mF cm^{-2}	163.2 μW cm^{-2}	3.6 μWh cm^{-2}
CuO PPy[7]	Cu wire Carbon fiber	PVA/KOH	1.3V	/	39.67 mF cm^{-2}	/	9.31 μWh·cm^{-2}
Co_3O_4@MnO_2 Graphene[8]	Ni wire Carbon fiber	PVA/KOH	1.5V	0.1 mA cm^{-2}	13.9 mF cm^{-2}	75 μW cm^{-2}	4.34 μWh·cm^{-2}
MnO2[9]	AgNP/AgNW/ Au/ PVDF fibers	PVA/H_3PO_4	0.85V	0.1 mA cm^{-2}	24.5 mF cm^{-2}	10.6 μW cm^{-2}	0.63 μWh·cm^{-2}
RGO[10]	cotton yarn	PVA/H_2SO_4	1.0V	0.06 mA cm^{-2}	9.54 mF cm^{-2}	31.84 μW cm^{-2}	1.32 μWh·cm^{-2}
This work	CNT/aramid yarn	PVA/KOH	1.6V	0.5 mA cm^{-2}	526.64 mF cm^{-2}	401.49 μW cm^{-2}	151.67 μWh cm^{-2}

References

[1] C. Wei, Q. Xu, Z. Chen, W. Rao, L. Fan, Y. Yuan, Z. Bai, J. Xu, An all-solid-state yarn supercapacitor using cotton yarn electrodes coated with polypyrrole nanotubes, Carbohydr. Polym. 169 (2017) 50-57.

[2] H.-T. Wang, C. Jin, Y.-N. Liu, X.-H. Kang, S.-W. Bian, Q. Zhu, Cotton yarns modified with three-dimensional metallic Ni conductive network and pseudocapacitive Co-Ni layered double hydroxide nanosheet array as electrode materials for flexible yarn supercapacitors, Electrochim. Acta 283 (2018) 1789-1797.

[3] F. Su, X. Lv, M. Miao, High‐performance two‐ply yarn supercapacitors based on carbon nanotube yarns dotted with Co3O4 and NiO nanoparticles, Small 11(7) (2015) 854-861.

[4] T.S. Le, T.K. Truong, J. Bae, D. Suh, Synergetic design of enlarged surface area and pseudo-capacitance for fiber-shaped supercapacitor yarn, Nano Energy 67 (2020) 104198.

[5] C. Zhou, M. Hong, Y. Yang, C. Yang, N. Hu, L. Zhang, Z. Yang, Y. Zhang, Laser-induced bi-metal sulfide/graphene nanoribbon hybrid frameworks for high-performance all-in-one fiber supercapacitors, J. Power Sources 438 (2019) 227044.

[6] Y.-F. Wang, H.-T. Wang, S.-Y. Yang, Y. Yue, S.-W. Bian, Hierarchical NiCo2S4@ nickel–cobalt layered double hydroxide nanotube arrays on metallic cotton yarns for flexible supercapacitors, ACS Appl. Mater. Interfaces 11(33) (2019) 30384-30390.

[7] R. Zhang, C. Chen, H. Yu, S. Cai, Y. Xu, Y. Yang, H. Chang, All-solid-state wire-shaped asymmetric supercapacitor based on binder-free CuO nanowires on copper wire and PPy on carbon fiber electrodes, J. Electroanal. Chem. 893 (2021) 115323.

[8] X. Niu, G. Zhu, Z. Yin, Z. Dai, X. Hou, J. Shao, W. Huang, Y. Zhang, X. Dong, Fiber-based all-solid-state asymmetric supercapacitors based on Co 3 O 4@ MnO 2 core/shell nanowire arrays, J. Mater. Chem. A 5(44) (2017) 22939-22944.

[9] P.T. Nguyen, J. Jang, Y. Lee, S.T. Choi, J.B. In, Laser-assisted fabrication of flexible monofilament fiber supercapacitors, J. Mater. Chem. A 9(8) (2021) 4841-4850.

[10] L. Li, D. Du, C. He, L. Yu, W. Tang, S. Hu, X. Wang, Z. Fu, L. Xia, W. Xu, Cotton yarns decorated with hydrothermally reduced graphene oxide for flexible supercapacitors, Ind Crop Prod 205 (2023) 117547.